11-2-2009

The Use of Polyethyleneimine to Control the Growth-Front Morphology of Electrochemically Deposited Gold Nanowires for Engineered Nanogap Electrodes

Manuel DaSilva
Purdue University, mdasilva@purdue.edu

Matthew M. Schneider
Purdue University - Main Campus, mmschnei.purdue@gmail.com

Daniel S. Wood
Purdue University - Main Campus, dswood@purdue.edu

Bong Joong Kim
Purdue University - Main Campus, kim341@purdue.edu

E A. Stach
Birck Nanotechnology Center and School of Materials Engineering, *Purdue University*, eastach@purdue.edu

See next page for additional authors

The Use of Polyethyleneimine to Control the Growth-Front Morphology of Electrochemically Deposited Gold Nanowires for Engineered Nanogap Electrodes

*Manuel DaSilva, Matthew M. Schneider, Daniel S. Wood, Bong-Joong Kim, Eric A. Stach, and Timothy D. Sands**

Porous anodic alumina (PAA) has generated increasing attention over the past decade for its use as a sacrificial template in the electrochemical synthesis of high-aspect-ratio nanomaterials.[1–4] However, a significant challenge that still remains unsolved concerns the control over the shape of the growth front of electrodeposited materials in a PAA template. The consensus of the molecular electronics community holds that many of the inconsistencies in the transport properties observed from a particular molecular device could be mitigated by better contact between the electrodes and molecule(s) of interest.[5–8] In such cases, it becomes imperative that the contact interfaces on both sides of the molecular layer be flat on the molecular scale. This requirement is particularly relevant to ''on-wire lithography'' (OWL), where the inner segment of a tri-layered electrodeposited nanowire is selectively etched to achieve a nanogap of equivalent dimensions.[9–13] The flat electrode surfaces could be expected to enable consistent measurements that would advance our understanding of the electrical characteristics of molecular systems. Similarly, the performance of a nanogap plasmonic antenna is sensitive to the shape of the metallic features and the gap between them.[14,15]

The difficulty in achieving surface planarization at the growth front of an electrodeposited nanowire may be attributed, in part, to surface characteristics of the PAA template. The pore walls of PAA contain a high concentration of oxygen vacancies that lend to its positively charged surface.[16] This charge imbalance is compensated by the adsorption of hydroxylated anions, which provides the PAA template with its hydrophilic property.[17] The presence of hydroxyl groups within the interior pore walls of a PAA template favors the formation of nanowires that possess non-planar growth fronts at slow to moderately high nanowire growth rates, or under non-equilibrium growth conditions.[18] At relatively fast nanowire deposition rates, the strong hydrophilicity of PAA can be circumvented by decreased lateral diffusion of the ionic species along the deposition interface. This improvement will, however, occur at the expense of grain size reduction[19] and a broadened distribution in the lengths of the nanowires.

Historically, PEI has been utilized as a brightening agent in plating solutions for improving the surface finish and grain structure of electrodeposits.[20,21] In industrial manufacturing, PEI is an important additive for increasing the speed of electroplating, enhancing efficiency, and reducing stress buildup of large-area metallic films.[22] More recently, the self-adsorbent property of a highly branched PEI has been used to improve the surface characteristics of PAA.[23] The present study was conducted to further investigate the role of PEI on nanowire growth. Here, the aliphatic amine was added directly to Orotemp-24 (Technic Inc.), a gold-plating electrolyte, rather than being incorporated onto the side walls of the PAA template as in the work by Moon et al.[23] The aim of this research was to achieve planarization at the growth front and minimize the distribution of length in the nanowire array without adversely affecting the microstructure of the as-deposited Au nanowires.

Two sets of control studies were performed; one to investigate the effect of the molecular weight of PEI and the other to examine the influence of the concentration of PEI on the electrochemical growth of Au nanowires in PAA. A field-emission scanning electron microscopy (FESEM) image of the

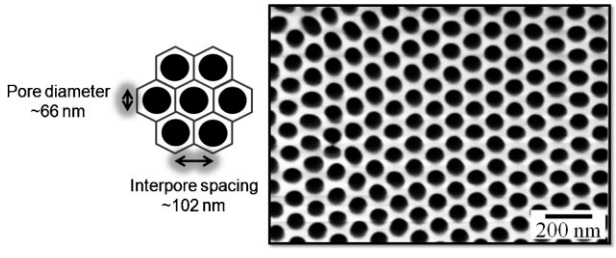

Figure 1. FESEM image of top surface of PAA template.

[*] Prof. T. D. Sands, Dr. M. DaSilva,[+] M. M. Schneider, D. S. Wood, Dr. B.-J. Kim, Prof. E. A. Stach
Birck Nanotechnology Center and
School of Materials Engineering
Purdue University
West Lafayette, IN 47907 (USA)
E-mail: tsands@purdue.edu
Prof. T. D. Sands
School of Computer and Electrical Engineering
Purdue University
West Lafayette, IN 47907 (USA)
[+] New address:
Morgan Electro Ceramics
232 Forbes Road, Bedford, OH 44146 (USA)

DOI: 10.1002/smll.200900379

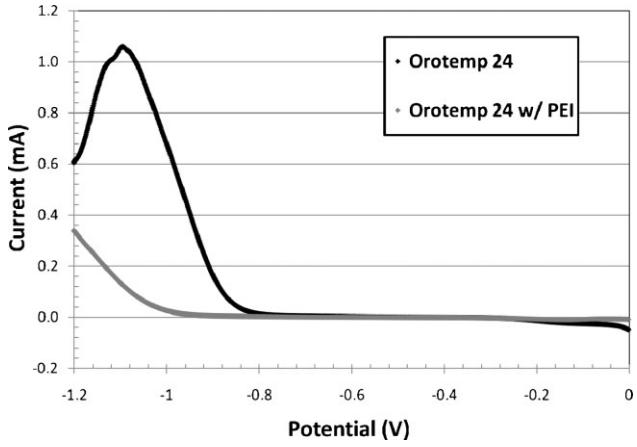

Figure 2. Voltammogram showing the reduction behavior of Orotemp-24, and the same electrolyte containing 3.2 wt% (600 amu) PEI. The voltammogram was performed at a sweep rate of 0.15 mV s^{-1} (versus Ag/AgCl) on a 21.5-μm-thick PAA template having a pore diameter of ≈66 nm and interpore spacing of ≈102 nm. The lateral area of the PAA template (after correcting for a 38% porosity) exposed to the underlying tungsten back electrode was 0.023 cm^2.

top surface of the PAA template is shown in Figure 1. A linear voltammogram was recorded to investigate the electrochemical behavior of Orotemp-24, and another for the Orotemp solution containing 3.2 wt% (600 amu) PEI. According to the voltammogram (Figure 2), the first appreciable sign of Au^+ reduction current occurs near −0.80 V for the electrolyte that contained no PEI. At this potential, the electrochemical reaction is under kinetic control since the concentration of ions within the bulk electrolyte is similar to the concentration near the deposition interface. Under this condition, the reduction rate will have an exponential dependence with increasing (more negative) potential. As the potential nears −0.95 V, the system is in a mixed kinetic and mass-transport regime since a concentration gradient exists within the long and narrow pores of the PAA template. This combination of growth modes is favorable for the formation of Au nanowires having dense bamboo-shaped grains.[19] For the Au electrolyte containing 3.2 wt% of the 600 amu PEI, a kinetically dominated reduction process of the ionic species begins at ≈−0.95 V. The peak shift observed in the voltammogram is indicative of the suppression in the reduction behavior of Au^+ caused by PEI.

The addition of PEI played a significant role in the electrochemical growth process. Au nanowires electrodeposited for 2 h at −0.95 V from the electrolyte that contained no PEI grew at a time-averaged growth rate of 0.30 nm s^{-1}, and had a standard deviation in length of 11.0%. The broad distribution in nanowire length is representative of a mass-transport-limited growth process. The Au ions travel great distances relative to their ionic size before they are reduced at the deposition interface. This long pathway for the ionic species within the PAA template introduces variance in the total number of Au^+ each pore receives over the two-hour deposition time, leading to a relatively large distribution of lengths of the nanowires. The broad distribution of nanowire lengths is also attributed to the high stability of the aurocyanide complex, which causes reduction to occur at more negative potential.[24] This condition hinders the possibility for homogenous filling of metal in the pores, as there will be a strong tendency for decomposition of water and formation of hydrogen gas in the electrolytic bath. Consequently, the electroplating efficiency (defined in this context as the percentage of electrons consumed by metal ions at the reaction interface as compared to the total number of electrons supplied to the working electrode) is reduced when Au is deposited from a cyanide-based electrolyte. Furthermore, the formation of hydrogen gas bubbles attracted to the surface of the template may also prohibit the uniform flow of metal ions into the pores. Consequently, the time-averaged electroplating efficiency of Au nanowires grown from Orotemp-24 at −0.95 V for 2 h was 5.8%. The growth front of the Au nanowires grown from the electrolyte that contained no PEI was non-planar. The nanowires exhibited a dense microstructure, and maintained a diameter consistent with the 66 ± 5-nm pore diameter of the PAA template. The growth rate of Au was substantially reduced for the electrolytes containing PEI (Table 1a). The reduced growth rate is attributed to the suppression in the reduction behavior of Au^+ caused by PEI. (This behavior of PEI has also been reported for ZnO nanowires synthesized by a non-electrolytic seeded growth technique.[25]) The suppression in the reduction behavior of Au^+ resulted in improved electroplating efficiencies (>30%), and provided improved uniformity in the total amount of ions each pore received over the deposition cycle ($\sigma_{rel} = 7.5\%$). Planarization of the nanowire growth front was greatest for the electrolyte that contained 600 amu PEI (Figure 3). This electrolyte also resulted in the narrowest distribution in nanowire lengths ($\sigma_L = 75$ nm). Figure 3 summarizes the distributions in Au nanowire lengths with varying molecular weight of PEI.

In a second study, the effect of concentration of 600 amu PEI on Au nanowire growth was examined. The Au nanowires grown from the electrolyte containing 3.2 wt% PEI exhibited superior surface planarization over those grown at higher concentrations (Figure 3). An increased concentration of PEI resulted in reduced nanowire growth rates but yielded concave

Table 1. Growth analysis for Au nanowires deposited from electrolytes containing different molecular weight of PEI. Concentration of PEI = 3.2 wt%.

	w/o PEI	600 amu PEI	1800 amu PEI	10000 amu PEI
Applied potential [mV]	−950	−950	−950	−950
Current density [mA cm^{-2}]	5.1	0.36	0.28	0.27
Mean nanowire length [μm]	2.18	1.00	0.71	0.69
Plating efficiency [%]	5.8	36.8	34.4	33.2
Growth rate [nm s^{-1}]	0.30	0.14	0.099	0.096
Standard deviation, σ [nm]	240	75	80	80
Relative deviation [% mean length]	11.0	7.46	11.27	12.38

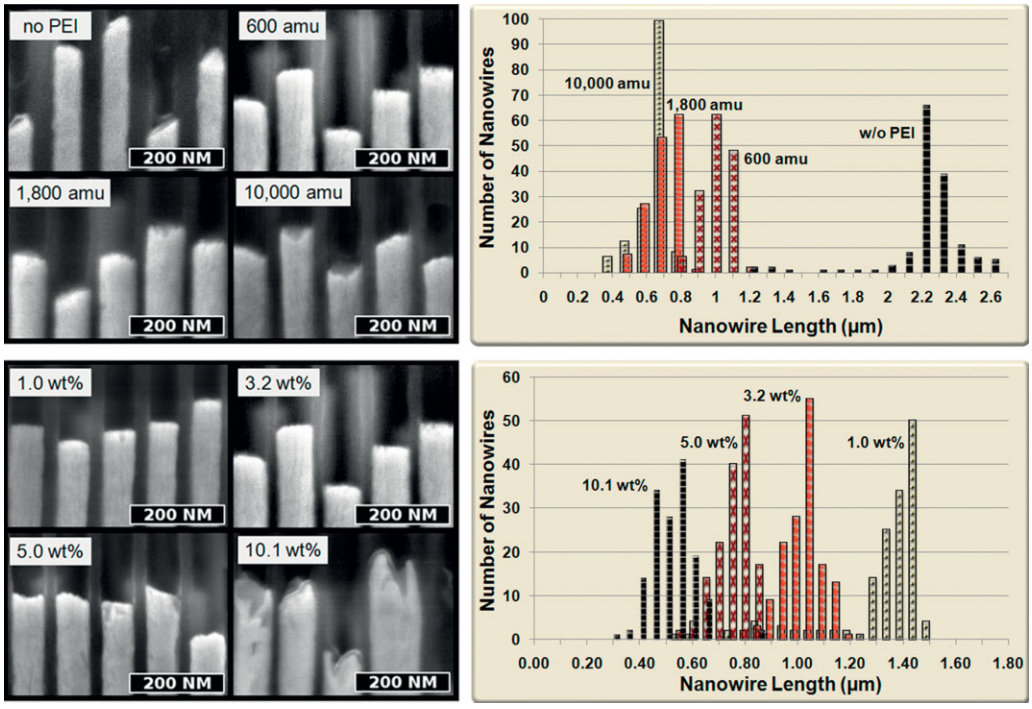

Figure 3. FESEM images of representative growth fronts as a function of molecular weight (top left) and concentration (bottom left) of PEI. The corresponding histograms (top right and bottom right) show the length distributions of nanowires as determined by FESEM.

nanowire growth fronts. This morphology is in stark contrast to the convexity observed in the nanowires grown without PEI at −0.95 V. The electrolyte composed of 1.0 wt% of 600 amu PEI resulted in the highest degree of planarization in the nanowire growth fronts but also favored a broadened nanowire length distribution (Figure 3 and Table 2).

Based on the results reported here, an electrolyte composed of Orotemp-24 and 3.2 wt% of 600 amu PEI was suitable for the combination of planarized nanowire growth fronts and minimization of the distribution in nanowire lengths. The Au nanowires were characterized by transmission electron microscopy (TEM) to confirm the morphology existing at the deposition interface. In Figure 4, the growth direction of a gold nanowire electrodeposited at −0.95 V without PEI was ⟨110⟩ with a strong facet near the top portion of the nanowire, suggesting that two {111} growth faces may be conjoined at the center. This microstructure was typical of the majority of nanowires grown at these conditions. A gold nanowire electrodeposited with PEI is also shown in Figure 4. The nanowire is dense and polycrystalline. The grain size near the tip of the nanowire varies from 20–95 nm in the radial direction and from 60–470 nm along the growth direction of the nanowire. In agreement with FESEM results, the nanowires synthesized from the electrolyte containing PEI had improved planarity over those grown without PEI.

The degree of planarization in the nanowire growth front was quantified using MATLAB. Figure 5 shows a set of FESEM images taken of nanowires grown without PEI (left) and those grown with 3.2 wt% of 600 amu PEI. The nanowire tips were identified as a local extrema of the image's horizontal gradient. The computation of the numerical derivative as a function of axial position yielded the relative extremum to a single point. This procedure was repeated for each position perpendicular to the nanowire axis to determine the co-ordinates for the entire nanowire edge in projection. Following the acquisition of this data, a simple ''planarization parameter'' was computed by taking the average difference between the projected peaks and valleys divided by the mean nanowire diameter (as determined by FESEM in projection). For the cases of Au nanowires grown without PEI, and those grown with 3.2 wt% of 600 amu PEI, the growth front ''planarization parameter'' was 0.14 and 0.35, respectively.

Table 2. Growth analysis for Au nanowires deposited from electrolytes containing different concentrations of PEI. Molecular weight of PEI = 600 amu.

	w/o PEI	1.0 wt% PEI	3.2 wt% PEI	5.0 wt% PEI	10.1 wt% PEI
Applied potential [mV]	−950	−950	−950	−950	−950
Mean nanowire length [μm]	2.18	1.31	1.00	0.73	0.49
Growth rate [nm s^{-1}]	0.30	0.18	0.14	0.10	0.068
Standard deviation, σ [nm]	240	180	75	66	82
Relative deviation [% mean length]	11.0	13.8	7.5	9.0	16.8

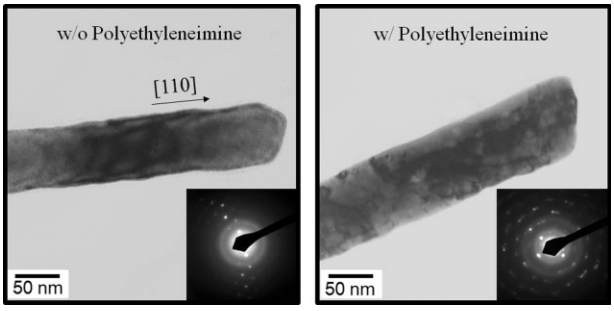

Figure 4. Bright-field TEM images of Au nanowires grown with Orotemp-24 (left), and the same containing 3.2 wt% 600 amu polyethyleneimine (right). Diffraction patterns taken from the top portion of the nanowires are shown in the inset.

To demonstrate the effectiveness of PEI on the planarization of nanowire growth fronts, multicomponent Au–Ag nanowires were synthesized in ≈70-nm-pore-diameter PAA templates. Constant potential was applied during the deposition of Au (−950 mV) and Ag (−500 mV) layers using a dual bath electrolytic system. The first Au segment was deposited for 2 h while subsequent Au segments lasted 8 min. The first, second, and third Ag segments were deposited for 5, 3, and 1 s, respectively. Figure 6 shows a representative FESEM image of the multicomponent nanowires in a PAA template. The junctions of the individual Au–Ag nanowire segments exhibit a high order of surface flatness compared to those grown without PEI. The longest Ag segment is ≈8 nm while subsequent layers have lengths that are proportionally smaller in size with decreasing deposition time. The images on the right of Figure 6 show the Au nanowires after a 5-min selective chemical etch of the Ag segments in nitric acid. The dimensions of the gaps are preserved following the completion of the Ag etching treatment.

The purpose of this study was to examine the effect of concentration and molecular weight of PEI on the electrochemical growth of Au nanowires. The studies reveal optimal surface planarization and nanowire growth rate uniformity for the electrolyte containing 3.2 wt% 600 amu PEI. Using this electrolyte, multicomponent Au–Ag nanowires were grown in sub-100-nm-diameter PAA templates. After etching of the Ag layers, sub-10-nm gaps were preserved between adjacent Au segments. The surface flatness at the junctions is improved as compared to the same nanowires grown without PEI.[9–13] The benefit of surface flatness at a nanowire growth front is important in molecular electronics where contact between a self-assembled molecule and source/drain electrodes is paramount. Similarly, smaller nanowire diameters can be beneficial in reducing the number of molecules confined within the gap and further our understanding of the transport characteristics of single molecules. The controlled electrochemical growth of tunable nanowire segments in sub-100-nm-diameter PAA templates remains a challenge but can be ameliorated by small additions of PEI to an electrolytic system.

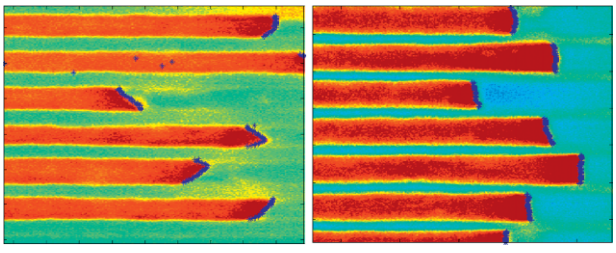

Figure 5. FESEM images of Au nanowires grown with Orotemp-24 (left), and the same containing 3.2 wt% 600 amu PEI (right). The color of the images is related to the intensity at a particular pixel.

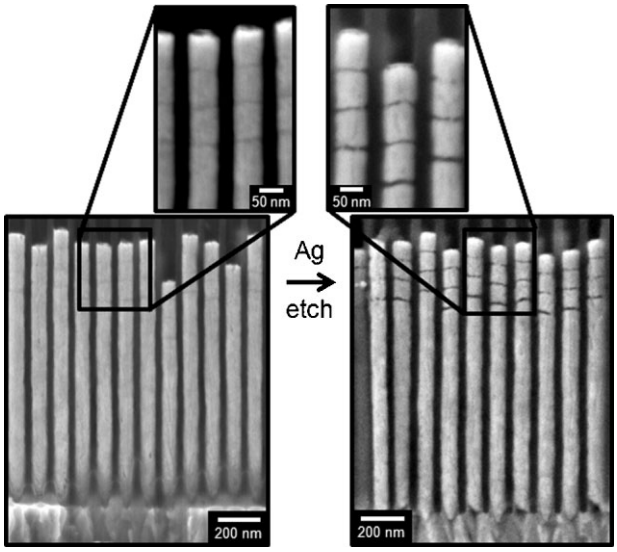

Figure 6. FESEM image of multicomponent Au–Ag nanowires in PAA template before and after Ag etch in nitric acid.

Experimental Section

Synthesis of PAA Templates: Aluminum foil (250 μm thick and 99.999% pure) was electropolished for 90 s at 20 V in 5 vol% sulfuric acid, 95 vol% phosphoric acid, and 20 g L^{-1} chromic (IV) oxide. A three-step anodization of Al was carried out at 40 V in 0.42 M oxalic acid at 1 °C. Pt gauze served as a counter electrode and was positioned 3 cm from the Al foil. The first, second, and third anodization steps were performed for 11.0, 5.0, and 4.5 h, respectively. The first and second anodized layers were removed in 3.5 vol% phosphoric acid and 45 g L^{-1} chromic (IV) oxide, at room temperature for 5 h. Removal of the residual Al separating the two stripes of PAA was achieved by submerging the sample in a concentrated solution of mercury dichloride and deionized water for 4 h. The barrier oxide layer residing at the base of the pores was removed in 1.9 wt% phosphoric acid for 15 min at 50 °C. Lastly, DC magnetron sputtering (100 Watts for 1350 s; 6 sccm Ar) was used to deposit 225 nm of W on one side of the 21.5-μm-thick PAA template, which served as the conducting layer for electrodeposition.

Synthesis of Nanowires: Electrochemical deposition was undertaken for the synthesis of nanowires in PAA templates. Orotemp-24 (Technic Inc.), containing 8.2 g L^{-1} Au^{+}, was used for the deposition of Au. PEI was added directly to the electrolyte, and stirred at room temperature for 15 min. Au nanowires were electrodeposited at −950 mV (versus Ag/AgCl) for 2 h. For

the synthesis of multicomponent Au–Ag nanowires, Au segments were electrodeposited at −950 mV from Orotemp-24 and 3.2 wt% of 600 amu PEI. Ag segments were electrodeposited at −500 mV from 6.4 mM silver sulfate, 0.46 M citric acid (monohydrate), and 1.08 M potassium thiocyanate. The first Au segment was deposited for 2 h, while subsequent Au segments lasted 8 min. The first, second, and third Ag segments were deposited for 5, 3, and 1 s, respectively. A cleaning procedure was performed after the completion of each metal segment to remove excess ions trapped from within the interior of the pores. This was achieving by immersing the PAA template in deionized water for 10 min in the presence of rigorous mixing by a magnetic stir bar. Etching of the Ag layers was accomplished by immersing part of a fractured PAA template in nitric acid for 5 min.

Keywords:

electrodeposition · molecular electronics · nanogap electrodes · nanowires · porous anodic alumina

[1] M. S. Sander, A. L. Prieto, R. Gronsky, T. Sands, A. M. Stacy, *Adv. Mater.* **2002**, *14*, 665.
[2] W. Lee, H. Han, A. Lotnyk, M. A. Schubert, S. Senz, M. Alexe, D. Hesse, S. Baik, U. Gosele, *Nat. Nanotechnol.* **2008**, *3*, 402.
[3] C. Ji, P. C. Searson, *Appl. Phys. Lett.* **2002**, *81*, 4437.
[4] W. Lee, R. Ji, U. Gosele, K. Nielsch, *Nat. Mater.* **2006**, *5*, 741.
[5] J. M. Seminario, *Nat. Mater.* **2005**, *4*, 111.
[6] M. A. Reed, *Proc. IEEE* **1999**, *87*, 652.
[7] F. Moresco, L. Gross, M. Alemani, K. H. Rieder, H. Tang, A. Gourdon, C. Joachim, *Phys. Rev. Lett.* **2003**, *91*, 036601.
[8] X. D. Cui, A. Primak, X. Zarate, J. Tomfohr, O. F. Sankay, A. L. Moore, T. A. Moore, D. Gust, G. Harris, S. M. Lindsay, *Science* **2001**, *294*, 571.
[9] S. Liu, J. B. H. Tok, Z. Bao, *Nano Lett.* **2005**, *5*, 1071.
[10] L. Qin, S. Park, L. Huang, C. A. Mirkin, *Science* **2005**, *309*, 113.
[11] B. Wildt, P. Mali, P. C. Searson, *Langmuir* **2006**, *22*, 10528.
[12] L. Qin, J. W. Jang, L. Huang, C. A. Mirkin, *Small* **2007**, *3*, 86.
[13] G. Zheng, L. Qin, C. A. Mirkin, *Angew. Chem. Int. Ed.* **2008**, *47*, 1938.
[14] P. Muhlschlegal, H. J. Eisler, O. J. F. Martin, B. Hecht, D. W. Pohl, *Science* **2005**, *308*, 1607.
[15] N. Yu, E. Cubukcu, L. Diehl, M. A. Belkin, K. B. Crozier, F. Capasso, D. Bour, S. Corzine, G. Hofler, *Appl. Phys. Lett.* **2007**, *91*, 173113.
[16] J. W. Diggle, T. C. Downie, C. W. Goulding, *Chem. Rev.* **1969**, *69*, 365.
[17] R. Redon, A. Vazquez-Olmos, M. E. Mata-Zamora, A. Ordonez-Medrano, F. Rivera-Torres, J. M. Saniger, *J. Colloid Interface Sci.* **2003**, *287*, 664.
[18] X. Dou, G. Li, H. Lei, *Nano Lett.* **2008**, *8*, 1286.
[19] M. Tian, J. Wang, J. Kurtz, T. E. Mallouk, M. H. W. Chan, *Nano Lett.* **2003**, *3*, 919.
[20] T. Iida, M. Yoshino, J. Sasano, I. Matsuda, T. Osaka, *J. Surface Finish. Soc. Japan* **2004**, *55*, 962.
[21] S. Masaki, H. Inoue, H. Honma, *Met. Finish.* **1998**, *96*, 18.
[22] W. A. Wilson, H. M. Hradil, E. F. Hradil, **1975, US Patent 3,864,222.**
[23] J. Moon, A. Wei, *J. Phys. Chem. B* **2003**, *109*, 23336.
[24] A. M. Sullivan, P. A. Kohl, *J. Electrochem. Soc.* **1997**, *144*, 1686.
[25] M. Law, L. E. Greene, J. C. Johnson, R. Saykally, P. Yang, *Nat. Mater.* **2005**, *4*, 455.

Received: February 28, 2009
Revised: June 15, 2009
Published online: August 6, 2009

